

# CNT-PDMS Nanocomposite for Energy Harvesting and Wearable Electronics Application

Ravi Patidar<sup>1</sup>, Anil Khandelwal<sup>2</sup>

<sup>1</sup>M.Tech Scholar, <sup>2</sup>Prof. & HOD

Department of electronics & communication Engineering, VNS Group of Institution, Bhopal, M.P.

**Abstract - Flexible wearable electronics are emerging field in the future technological advancement. Carbon nanotubes (CNT) are versatile material because of its tremendous electrical and mechanical characteristics. In this work, we have successfully prepared CNT- Polydimethyl siloxane (PDMS) composite for energy harvesting, using low cost spin coating method. The synthesized nanocomposite film is characterized by various characterization techniques, like X-ray diffraction (XRD), Fourier transform infrared spectroscopy (FTIR) and scanning electron microscopy (SEM). Dielectric constant was 30 at 20 MHz calculated at room temperature. The nanocomposite generated open circuit output voltage and short circuit current 4V and 60 nA, respectively by the application of mechanical force. The device can be utilized as sensor such as pulse detector, voice detector and mechanical sensor, etc.**

## I. INTRODUCTION

Carbon has been showing great potential to revolutionize many aspects of our life in the form of carbon nanotubes (CNTs) and graphene, the two latest emerging carbon allotropes, during the last two decades.[1, 2] CNTs and graphene exhibit the supreme electrical, thermal, optical and mechanical properties almost on the same level [3]. Flexible electronics is a technology for building electronic devices on flexible plastic substrates by a higher-throughput and lower-cost process compared to traditional rigid chips. The aim of flexible electronics is not to replace traditional silicon electronics, instead flexible electronics changes the basic requirement of 2D rigid substrates and enables the production of completely new flexible devices in a broad range of novel applications in flexible displays, energy storage and generation, intelligent interactivity etc. [4-8]. The breakthrough of carbon nanotubes has got remarkable progress in various fields of research and applications due to their peculiar structural, electrical, mechanical, optical and magnetic properties [9]. The diameter of CNTs is in the 1-100nm range and it can be up to millimeters long [10]. These dimensions lead to very high aspect ratios as compared to that of carbon fibers. This combination of properties allows better interaction in composite matrices, resulting in improved properties and performance [11].

The incorporation of CNTs into the polymer can enhance the properties of material by increasing

mechanical strength and electrical conductivity. However the formation of aggregates and low dispersions of CNTs in the polymer matrix are the major cause of poor and non-homogeneous composites[12]. The interface between the CNTs and the polymer matrix plays a vital role in achieving good dispersion. Successful incorporation of CNTs in polymer matrices could result in different types of lightweight and strong materials for flexible electronic devices and sensors [13].

## II. EXPERIMENTAL DETAILS

### Materials:

Multi-walled carbon nanotubes (MWCNTs, CM-95, >95.0%, 10–20-nm outer diameter, 10–20- μm length) were obtained from Hanwha Nanotech (Seoul, Republic of Korea). All PDMS components were purchased from Dow Corning (Midland, MI, USA). All chemicals, including IPA and other organic solvents, were obtained at high-performance liquid chromatography (HPLC) grades with >99.9% purities from Sigma-Aldrich (St. Louis, MO, USA).

### Fabrication of the CNT/PDMS Nanocomposites:

Pristine MWCNTs were first dispersed in IPA with a 100:1 weight ratio and ultrasonicated for 3 Hrs to obtain single CNTs dispersed in excess IPA solution. To obtain a homogeneous dispersion, 80 wt% of PDMS-A was added and ultrasonicated for 1 Hrs. After IPA was evaporated from the dispersion using a hot plate at 60 °C the, crosslinker PDMS-B was added and vigorously mixed. A vacuum desiccator was used to remove the bubbles remaining from the mixing process. The blend was cast in using a spin coating method and cured in an oven for 3 h at 90 °C.

### Characterization and measurement:

Crystalline phase and mineralogical studies was measured using X-ray diffraction (XRD) technique (Rigaku Mini Flex II) with Cu K $\alpha$  radiation ( $\lambda = 1.5401 \text{ \AA}$ ). Fourier-transform infrared spectroscopy (FT-IR) spectra of prepared CNT-PDMS composites were recorded in the

range of 500-3000  $\text{cm}^{-1}$  at 4  $\text{cm}^{-1}$  resolution using the Thermo Scientific Nicolet iS50 FT-IR spectrometer. Checking electron microscopy (SEM) (JEOL JSM 6360A) is utilized to contemplate the morphological properties. Dielectric steady and digression loss of tests were estimated utilizing an Agilent E4980A LCR meter at room temperature and recurrence scope of 20 Hz-2 MHz.

Piezoelectric yield voltage was estimated utilizing blended space oscilloscope (Model: Tektronix-MDO3052) and flow was estimated utilizing Keithley electrometer (Model: 6517B). The vertical power on the nanogenerator gadget was applied through the PC interfaced dynamic shaker utilizing The Modal Shop, Model: K2007E01 arrangement.

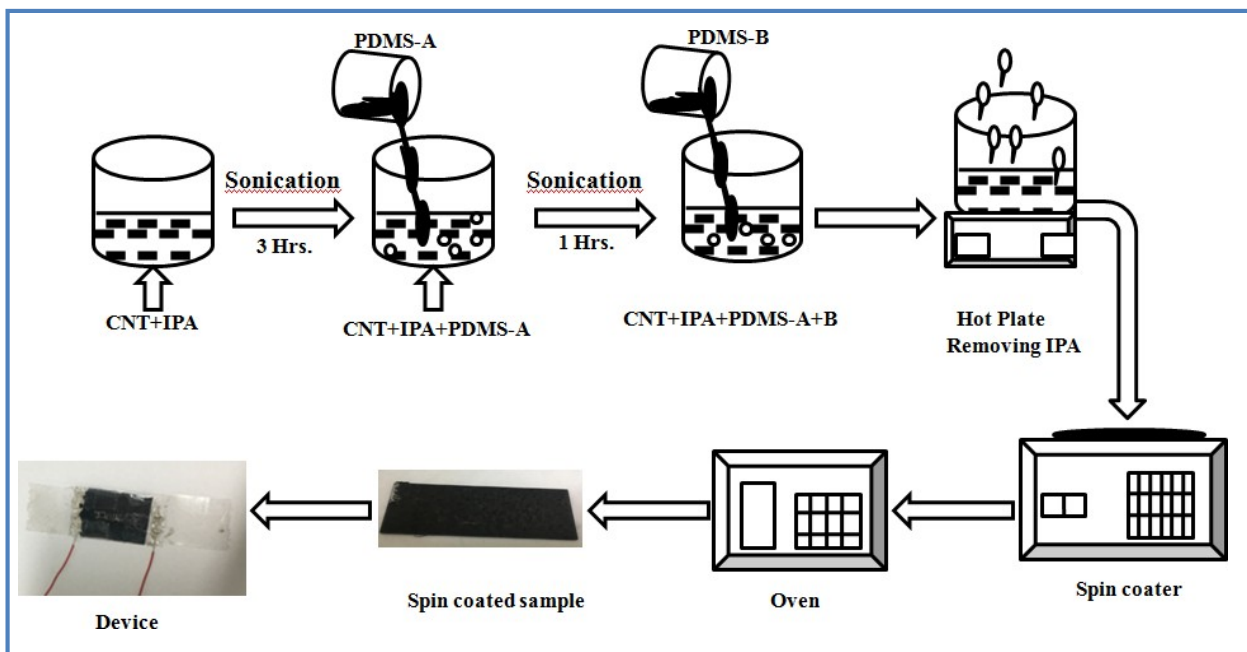


**Fig.1** Block Diagram of Fabrication of CNT/PDMS Nanocomposites

### III. RESULTS AND DISCUSSION

#### X-Ray diffraction analysis:

The X-ray diffraction (XRD) data for PDMS and CNT-PDMS composites are shown in Fig.2 Exhibiting relatively good crystalline structures. The CNT-PDMS composites show slight increases in diffraction peak intensities at approximately  $20^\circ$ , indicating a greater presence of carbon core structures in the composites.

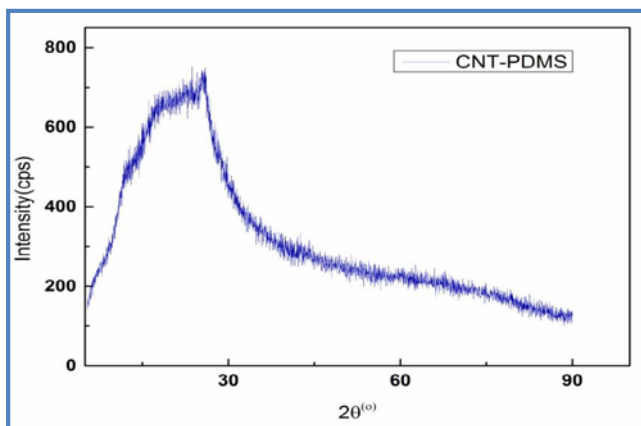


**Fig. 2** XRD results of CNT-PDMS Nanocomposite

The PDMS film exhibits two broad peaks at the  $2^\circ$  angles of  $\sim 21^\circ$  and  $\sim 26^\circ$ . When 4-wt% CNT is

incorporated into the PDMS, the peak at  $20^\circ$  becomes more intense than that of PDMS, possibly from the superimposition of peaks from PDMS and the CNTs. The decreased PDMS crystalline causes the XRD crystal peak to broaden.[14]

To evaluate the components of the boscage-like structure, the sample was characterized by X-ray diffraction patterns (XRD). Fig.2 Shows the XRD pattern of the laser-ablated surface of the composite sample. A strong diffraction peak centered at around  $2\theta$  angle of  $26.4^\circ$  can be observed, which is the characteristic peak of MWCNT [15] This indicates that the boscage-like structure mainly consisted of MWCNT. In addition, to analyze the phase composition of the products wrapped on the MWCNT, XRD was also employed to characterize the laser ablated surface of PDMS. The XRD spectra of PDMS show a diffuse peak at  $2\theta$  angle of  $21^\circ$ , which is in the matrix. Meanwhile, the amorphous carbon attached to the MWCNT may help to constitute the effective conductive networks, Due to the attached amorphous carbon, disconnected MWCNT are connected to form the sparse conductive network, and more tunneling effect sites are also created in the conductive networks, which may lead to

the high sensitivity of the composite strain sensor[16]

**Fourier transform-infrared spectroscopy (FT-IR) studies:**

**Fig.3** summarizes the positions of IR absorption bands of the chemical groups found in the PDMS- CNT composites. -CH<sub>3</sub> wagging related peaks is located at 1410 cm<sup>-1</sup> and at 1258 cm<sup>-1</sup>. A wide multi- component peak ranging from 1000 cm<sup>-1</sup> to 1100 cm<sup>-1</sup> corresponding to symmetrical Si-O-Si stretching is also present. There is a minor decrease in the peak at 930 cm<sup>-1</sup> which shifts to lower wave numbers as the concentration of MWCNTs increase in PDMS. In addition the ratio between the two transmissions values at 900 cm<sup>-1</sup> and 930 cm<sup>-1</sup> decrease with increasing CNT content as shown in **Fig.3**. This is in good agreement with the literature [17, 18] as this effect is also observed for other carbon materials based composites. Si-C bands and rocking peaks for Si(CH<sub>3</sub>)<sub>2</sub> are observed in 835-855 cm<sup>-1</sup> and 785-815 cm<sup>-1</sup> regions, respectively [19-21]

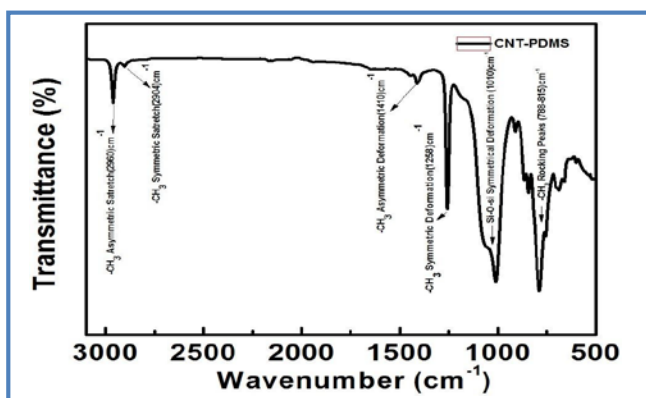


**Fig. 3** FTIR Spectra of CNT-PDMS Nanocomposite

**3.3SEM analysis:**

To study the morphology of the CNT-PDMS composite, scanning electron microscopy was investigated using JEOL-6000, Japan at 15 Kv. Thin film of composite was taken for analysis (figure no). The obtained results showed that CNT is well dispersed in the PDMS matrix which is further responsible for uniform surface structure.[22] The tubular structure of CNT (encircled with orange color) can be observed in **Fig.4(a)** however, some clusters (encircled with yellow color) formed due to agglomeration of nano tubes can also be observed.

Each CNT within a bundle is attached by the vander Waals interaction, as shown in the inset in **Fig.4 (d)** which is a typical SEM image of the as-produced CNTs. To maximize the composite's performance for a given CNT vol.20 %, the nano tubes must be separated and then dispersed within the polymer matrix while retaining a high aspect ratio.[ 23 , 24]

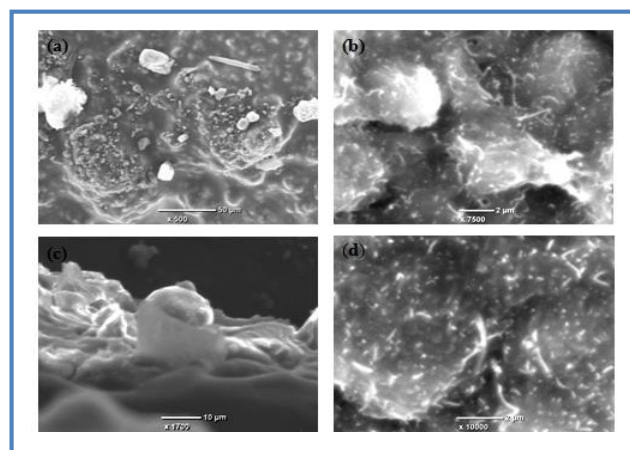


**Fig. 4** SEM analysis of CNT-PDMS nanocomposite. (a) & (b) matrix PDMS-CNT morphology. (c) & (d) at higher magnification clearly observed CNT-PDMS matrix

**Electrical and dielectric analysis:**

Impedance measurements are a powerful method of characterizing and modeling the electrical properties of materials and interfacial regions between different materials.[25] The fabricated CNT/PDMS Nanocomposites was fixed by using a vise apparatus with parallel metal plates, and its impedance characteristics were then obtained in the frequency range of 20 Hz-2 MHz, as shown in **Fig. 5(a-b)** represent the measured total impedance (Z) and phase angle (θ) as a function of frequency, respectively. The total impedance contains a real part (resistance) and an imaginary part (reactance), and the phase angle can be given as tan(reactance/resistance), which denotes phase shift between voltage and current signals.

The obtained result were plotted between logarithm of Z modulus and logarithm of the applied frequency shown in **Fig.5(a)** and Z phase and logarithm of the applied frequency shown in **Fig.5(b)** to confirm the nature of internal electrical impedance of the device. The impedance slope was calculated and found to be - 0.99 which proves a capacitive response of the well- known nanogenerator. The - 90 phases, as obtained from the Z phase curve **Fig. 5(b)** further confirms the capacitive response of the device. These results were in good agreement with the previous reported result of piezoelectric nanogenerators.

Dielectric constant of the synthesized material was investigated at room temperature in the frequency range of 20Hz-20MHz.

Dielectric constant of the synthesized material was investigated at room temperature in the frequency range of 20Hz-20MHz.

Dielectric constant (ε) of the materials was calculated by the relation [26]:

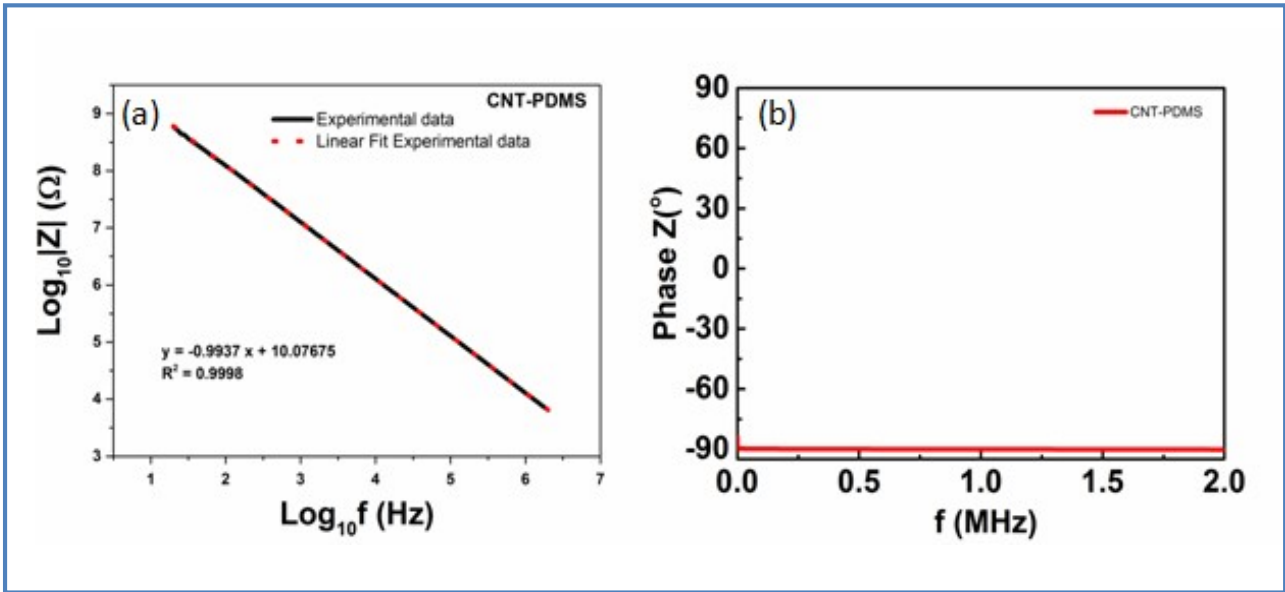


Fig. 5 (a) electrical Impedance. (b) Phase of CNT-PDMS Nanocomposite.

$$\epsilon_r = \frac{C_p * t}{\epsilon_0 * A}$$

Where,

$\epsilon_0$  = permittivity of free space, t = thickness of the sample

A = area of the sample

$C_p$  = capacitance of the sample

The value of dielectric constant comes out to be 30 at low frequency. It remains almost constant for entire range of frequency as shown in Fig.6 (a). In the high frequency region there is a small decrease in the value of dielectric constant. At low frequency, electric dipoles may move and follow the applied ac electric field, however as the

frequency increases but the dipoles are unable to follow the ac electric field frequency and lag behind the electric field resulting in decrease of dielectric constant. Moreover, the exponential decrease in the value of dielectric constant with increasing frequencies may be also attributed to a combined contribution of polarization such as ionic, electronic and interfacial[27-29]. In Fig.6 (b).The variation of dielectric loss tangent ( $\tan \delta$ ) with applied frequency in range of 20 Hz-2 MHz. Dielectric loss tangents shows similar trend.

A very low dielectric loss of value 0.010 at low frequency was observed but at high frequency region dielectric loss becomes very low and approaches to negative value of -0.010.

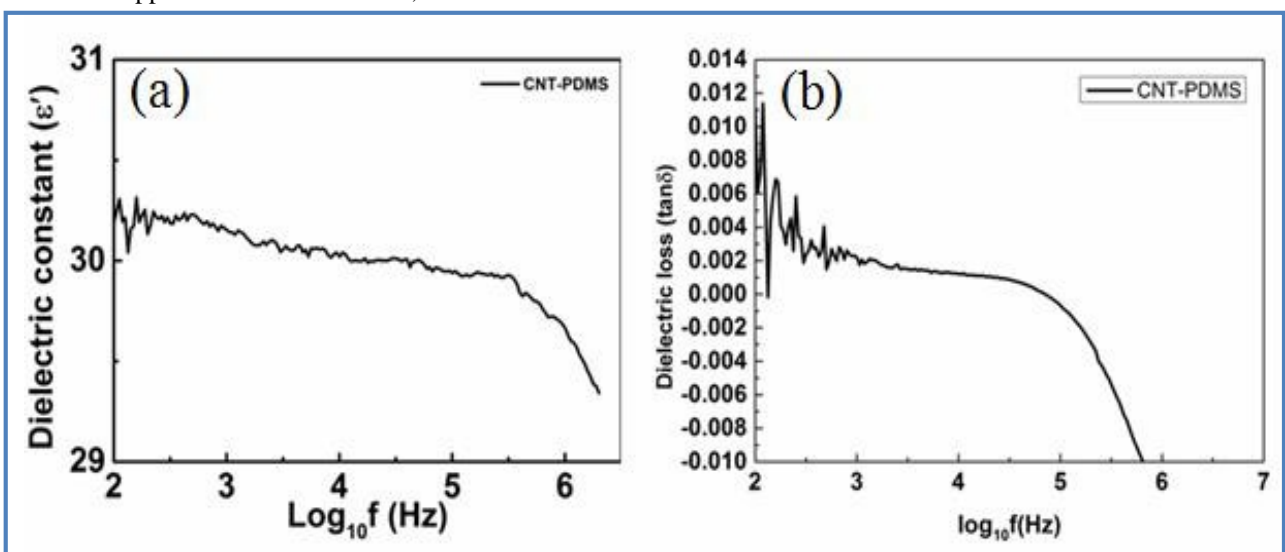


fig. 6.(a)Dielectric constant and (b) Dielectric loss of CNT-PDMS Nanocomposite

**Device operation:**

The working mechanism of the CNT/PDMS

Nanocomposites under vertical pressure can be understood by the generation of electric charges on the top and bottom surface of the device as shown in Fig.7 (a-c). When

mechanical pressure is applied, the piezoelectric induced electric field is induced on the top surface of the electrode towards silver electrode and positive potential induced on the bottom electrode of the device (ITO side), which results in induction of the potential difference between two electrodes. Due to this potential difference, the piezoelectric potential-driven electrons flow from top electrode to the bottom electrode and a positive electric

pulse was detected. On the other hand, when the external pressure is released, the piezoelectric potential disappears and accumulated electrons at bottom side flow and an electric signal in the opposite direction is detected as shown in Fig.7c. Moreover, present CNT create dipoles due to thermal vibration of the charge carrier on the application of external pressure to the CNT-PDMS nanocomposite device.

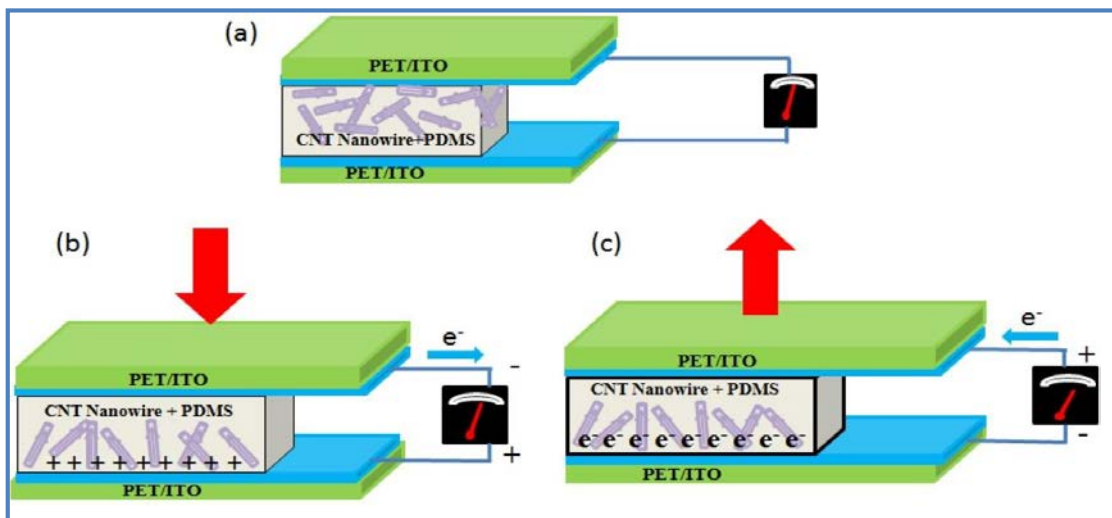


**Fig.7** Working mechanism of the CNT/PDMS

nanocomposites. (a) No piezoelectric output electric is generated in the absence of any mechanical strain. (b) Under vertical compression of the device, the piezoelectric potential induced electron flow from the top electrode to the bottom electrode side through the external load. (c) As the compressive strain is removed, the piezoelectric potential inside the device instantly disappears, the accumulated electron from the bottom electrode move back to the top electrode and an electric signal is observed in opposite direction.

**Output performance of the CNT-PDMS nanocomposite**

**device:**

**Energy harvesting Application:**

To fabricate the CNT-PDMS composite device, the CNT-PDMS thin film are spin coated based on the transparent and flexible ITO coated PET substrate and after crystallization, The bottom substrate ITO also acts as bottom electrode. To complete the fabrication of the piezoelectric nanogenerator, conducting silver electrode was coated as top electrode. The schematic image of device structure and original image of the nanogenerator is shown in the Fig.8.

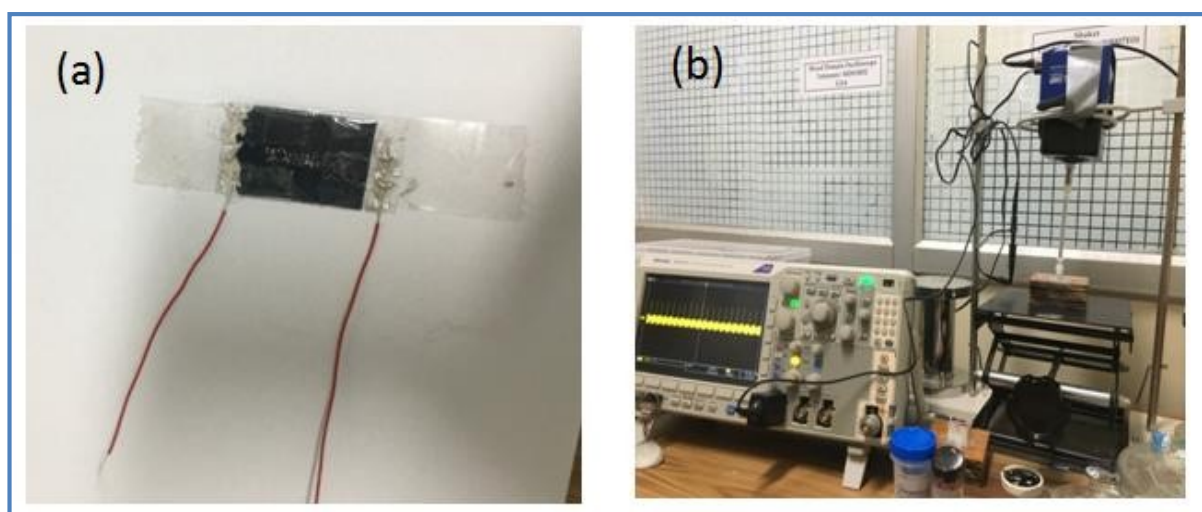


**Fig.8** (a) Original device image (b) Energy measurement set up of CNT-PDMS Nanocomposite.

The piezoelectric output voltage and current from CNT-PDMS nanogenerator were measured under vertical pushing and releasing conditions using computer controlled force simulator. The observed output voltage and current measured from the hybrid nanogenerator under controlled

Force of 0.05 kgf is shown in the Fig.9&10. A large output voltage of 4V and current of 60nA were obtained under vertical compression force as shown in the Figure respectively.

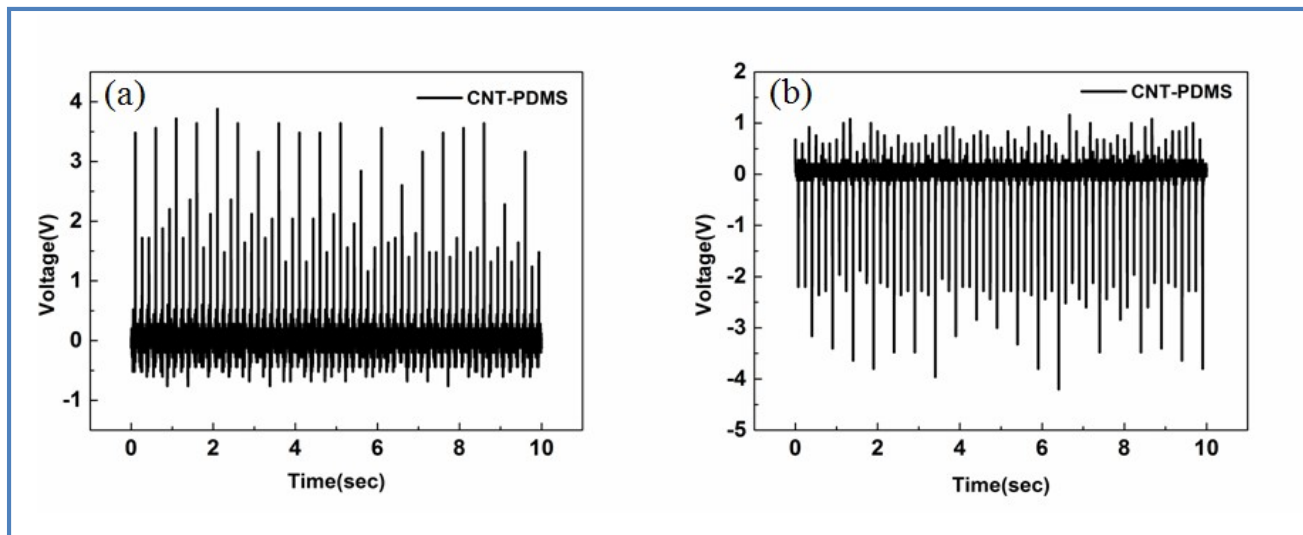


**Fig. 9.** (a) Open circuit forward voltage. (b) Open circuit reverse voltage of CNT-PDMS Nanocomposite.

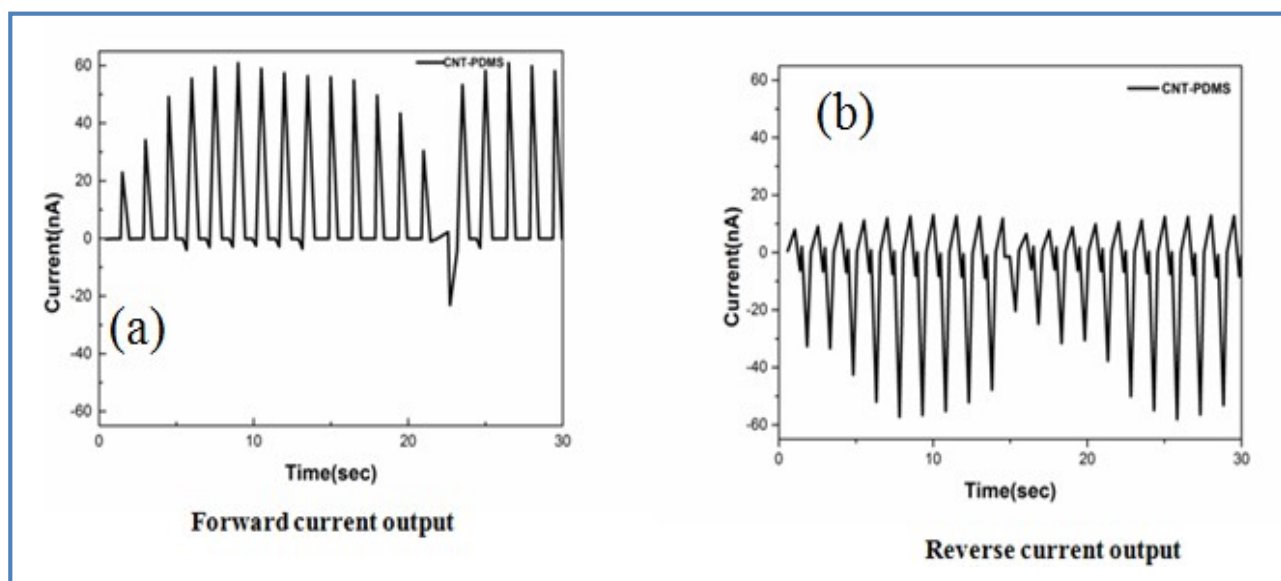


**Fig.10.** (a) Short circuit forward current. (b) Short circuit reverse current of CNT-PDMS Nanocomposite.

Switching-polarity test were also carried out to confirm that the output voltage and current originated from the piezoelectric phenomenon not from the equipment. An opposite output signal is observed when the device is connected in reverse connection.

**Motion sensor Application:**

In this study the device will be attached in my right hand. The device will be attached in mixed Domain Oscilloscope (Tektronix-MDO3052 USA) for check the output generated in device. The piezoelectric output voltage generated by CNT-PDMS Nanocomposites film by elbow movement

goes found to be of magnitude 2V **Fig.11(a)** depicts the graph between voltage and time that was produce by the motion of are elbow. Forward and backward movement shows corresponding positive and negative peaks of voltage respectively so it can be used as a motion sensor.

**Pulse detector Application:**

The piezoelectric output voltage generated by CNT-PDMS nanocomposite film by hand pulse movement was found to be of magnitude 1.5 V. **Fig.12** Depicts the graph between voltage and time that was produce by the motion of the pulse. Quite a good amount of piezoelectric output voltage

of magnitude 1.5 in both the directions was obtained. However, a lot of noise signal was also produced may be due to the environmental conditions. Hence this can be

used as a pulse sensor which can detect the presence of pulse in living human beings which can be very crucial in some situations of life.

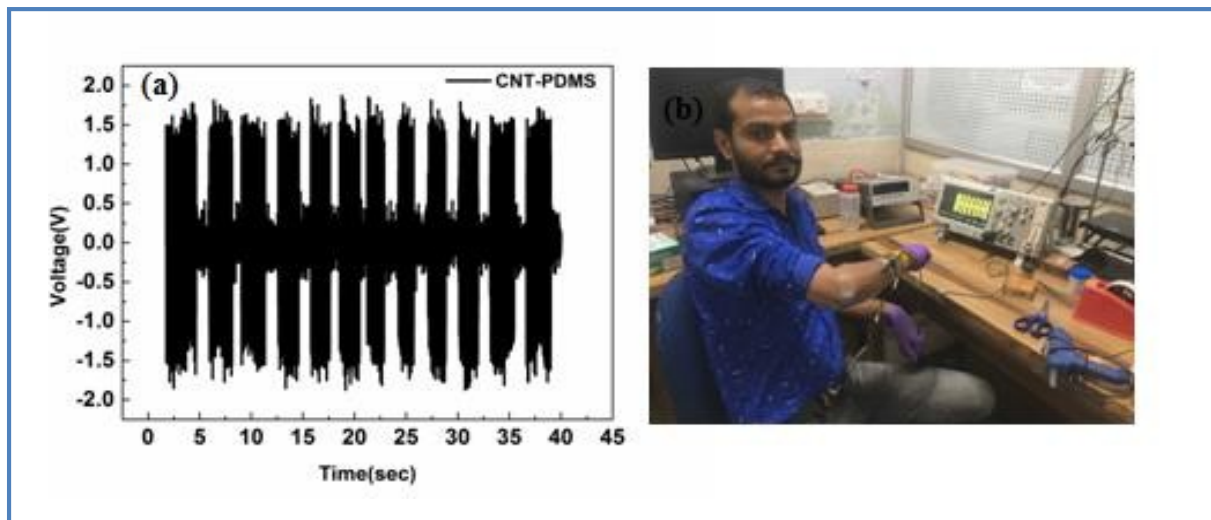


**Fig.11.** (a) Motion sensors response of CNT-PDMS nanocomposite device. (b) Real time picture of Measurement during elbow movement.

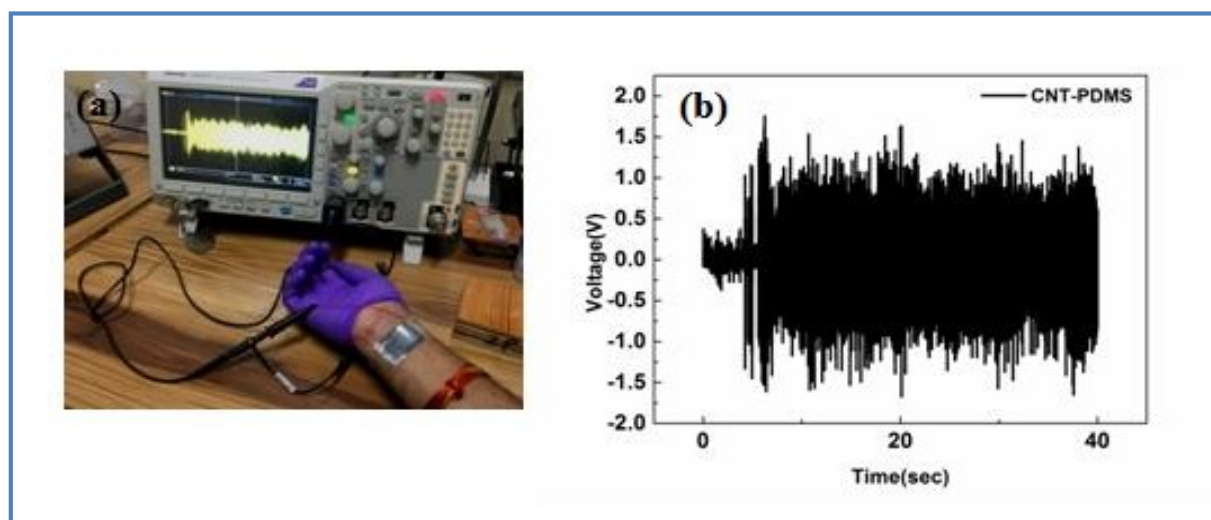


**Fig.12.** (a) Real time picture of Pulse detector. (b) Response of pulse of CNT-PDMS nanocomposite device.

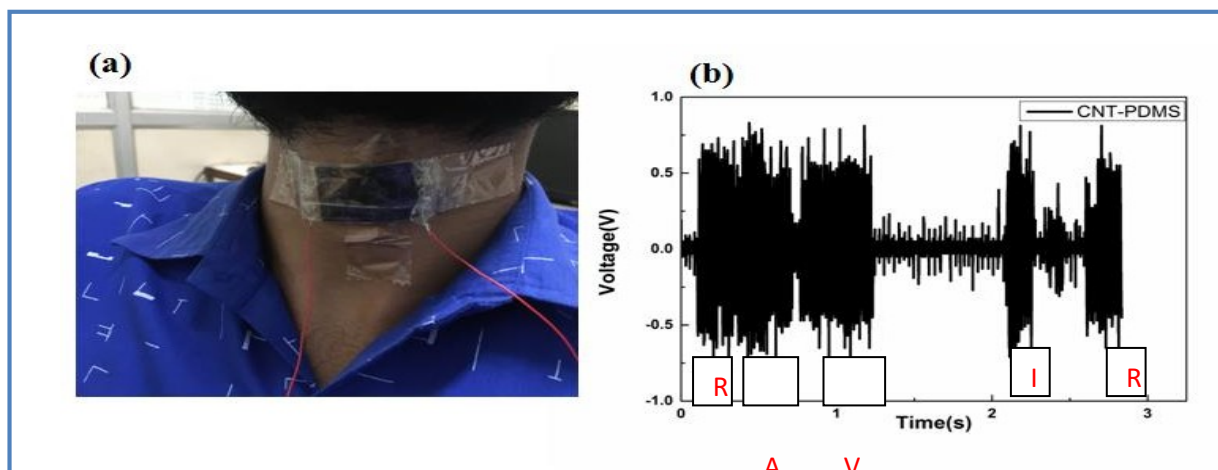


**Fig.13.** (a) Real time picture of Voice detector. (b) Response of pulse of CNT-PDMS nanocomposite device.

### Voice Detector Application:

The device can also be used as voice detector. We have placed the device on our throat and spoke some words like 'Ravi' as shown in fig.13 (b). The modulation in the voice was detected

in the form of output voltage generated. An output voltage as a function of time of magnitude  $\sim 1$  V was obtained. These results were in good agreement with the previous reported result of piezoelectric nanogenerators.

### IV. CONCLUSION

The CNT-PDMS composites show slight increases in diffraction peak intensities at approximately  $20^\circ$ , indicating a greater presence of carbon core structures in the composites. The SEM micrographs showed that CNT is well dispersed in the PDMS matrix which is further responsible for uniform surface structure. The  $-90^\circ$  phases, as obtained from the Z phase curve further confirms the capacitive response of the device. The value of dielectric constant comes out to be 30 at low frequency. It remains almost constant for entire range of frequency. The working mechanism of the CNT/PDMS Nanocomposites under vertical pressure can be understood by the generation of electric charges on the top and bottom surface of the device. Forward and backward movement shows corresponding positive and negative peaks of voltage respectively so it can be used as a motion sensor. This can be used as a pulse sensor which can detect the presence of pulse in living human beings which can be very crucial in some situation of life. The modulation in the voice was detected in the form of output voltage generated. The nanocomposite generated open circuit output voltage and short circuit current 4 V and 60 nA, respectively by the application of mechanical force. The obtained results are the new way to utilize to light up of the LED and also to utilize in wearable electronics application in near future.

### V. REFERENCES

- [1] Iijima, S., *Nature* 354 56 Iijima S and Ichihashi T 1993. *Nature*, 1991. 363: p. 603.
- [2] Novoselov, K.S., et al., *Electric field effect in atomically thin carbon films*. *science*, 2004.306(5696): p. 666-669.
- [3] 中西毅, R. Saito, G. Dresselhaus and MS Dresselhaus, *Physical Properties of Carbon Nanotubes*, Imperial College Press, London, 1998, xii+ 259p., 22× 15.5 cm, \10,560 [学部・大学院向, 専門書]. *日本物理学会誌*, 1999. 54(10): p. 832-833.
- [4] Kim, T.W., et al., *Electrical memory devices based on inorganic/organic nanocomposites*. *NPG Asia Materials*, 2012. 4(6): p. e18-e18.
- [5] Brosseau, C., *Emerging technologies of plastic carbon nanoelectronics: A review*. *Surface and Coatings Technology*, 2011. 206(4): p. 753-758.
- [6] Nathan, A., et al., *Flexible electronics: the next ubiquitous platform*. *Proceedings of the IEEE*, 2012. 100(Special Centennial Issue): p. 1486-1517.
- [7] Huang, X., et al., *Graphene-based materials: synthesis, characterization, properties, and applications*. *small*, 2011. 7(14): p. 1876-1902.
- [8] Liu, X., et al., *Large-scale integration of semiconductor nanowires for high-performance flexible electronics*. *ACS nano*, 2012. 6(3): p. 1888-1900.
- [9] Lau, K.T., M. Lu, and D. Hui, *Coiled carbon nanotubes: synthesis and their potential applications in advanced composite structures*. *Composites Part B: Engineering*, 2006. 37(6): p. 437-448.
- [10] Deck, C.P. and K. Vecchio, *Prediction of carbon nanotube growth success by the analysis of carbon-catalyst binary phase diagrams*. *Carbon*, 2006. 44(2): p. 267-275.
- [11] Coleman, J.N., et al., *Small but strong: a review of the mechanical properties of carbon nanotube-polymer composites*. *Carbon*, 2006. 44(9): p. 1624-1652.
- [12] Harris, P.J., *Carbon nanotube composites*. *International materials reviews*, 2004. 49(1): p.31-43.
- [13] Bakshi, S.R., D. Lahiri, and A. Agarwal, *Carbon nanotube reinforced metal matrix composites-a review*. *International materials reviews*, 2010. 55(1): p. 41-64.
- [14] Kim, J.H., et al., *Simple and cost-effective method of highly conductive and elastic carbon nanotube/polydimethylsiloxane composite for wearable electronics*. *Scientific reports*, 2018. 8(1): p. 1-11.
- [15] Cao, A., et al., *X-ray diffraction characterization on the alignment degree of carbon nanotubes*. *Chemical physics letters*, 2001. 344(1-2): p. 13-17.
- [16] Simmons, J.G., *Generalized formula for the electric tunnel effect between similar electrodes separated by a thin insulating film*. *Journal of applied physics*, 1963. 34(6): p. 1793-1803.
- [17] Nour, M., et al., *CNT/PDMS composite membranes for H2 and CH4 gas separation*. *International Journal of Hydrogen Energy*, 2013. 38(25): p. 10494-10501.
- [18] Nour, M., et al., *Nanocomposite carbon-PDMS membranes for gas separation*. *Sensors and Actuators B: Chemical*, 2012. 161(1): p. 982-988.
- [19] Maji, D., S. Lahiri, and S. Das, *Study of hydrophilicity and stability of chemically modified PDMS surface using piranha and KOH solution*. *Surface and Interface analysis*, 2012. 44(1): p. 62-69.
- [20] Agarwal, R., P. Tandon, and V.D. Gupta, *Phonon dispersion in poly (dimethylsilane)*. *Journal of Organometallic Chemistry*, 2006. 691(13): p. 2902-2908.
- [21] Shahzad, M., et al. *Study of carbon nanotubes based polydimethylsiloxane composite films*. in *Journal of Physics: Conference Series*. 2013. IOP Publishing.

- [22] Xu, W., et al., Micropatternable elastic carbon nanotube/PDMS electrets. *Power MEMS*, 2009: p. 4.
- [23] Chu, K., et al., Electrical and thermal properties of carbon-nanotube composite for flexible electric heating-unit applications. *IEEE Electron Device Letters*, 2013. 34(5): p. 668-670.
- [24] Nilchian, A. and C.-Z. Li, Mechanical and electrochemical characterization of CNT/PDMS composited soft and stretchable electrodes fabricated by an efficient solution-based fabrication method. *Journal of Electroanalytical Chemistry*, 2016. 781: p. 166-173.
- [25] Macdonald, J.R. and W.B. Johnson, Fundamentals of impedance spectroscopy. *Impedance spectroscopy: theory, experiment, and applications*, 2018: p. 1-20.
- [26] Wiser, N., Dielectric Constant with Local Field Effects Included. *Physical Review*, 1963. 129(1): p. 62-69.
- [27] Bharti, D.K., M.K. Gupta, and A.K. Srivastava, Giant dielectric constant and band gap reduction in hydrothermal grown highly crystalline zinc silicate nanorods. *Materials letters*, 2018. 232: p. 66-69.
- [28] Bharti, D.K., M.K. Gupta, and A.K. Srivastava, Temperature dependent dielectric and electric properties of zinc silicate nanorods. *Nano-Structures & Nano-Objects*, 2019. 17: p. 123-128.
- [29] Mondal, D., et al., Enhancement of  $\beta$ -phase crystallization and electrical properties of PVDF by impregnating ultra high diluted novel metal derived nanoparticles: Prospect of use as a charge storage device. *Journal of Materials Science: Materials in Electronics*, 2018. 29(17): p. 14535-14545.